Plasma Hydrogenation of High-Carbon Structural Steel Wires under Different Prestressing Levels

Amjad Saleh El-Amoush[a] (ID)*, Salman A. Al-Duheisat[b]*

[a]Al-Balqa Applied University, College of Engineering, Department of Materials and Metallurgical Engineering, 19117, P. O. Box 7181, Al-Salt, Jordan.
[b]Ajloun National University, College of Engineering, 26810, Ajloun, Jordan.

High-carbon structural steel wires were prestressed to various levels in a plasma hydrogenation environment and then pulled in a slow strain rate test (SSRT). The effect of plasma hydrogenation under different prestressing levels on the material's tensile response and hydrogen embrittlement was noted. It was found that the ultimate tensile strength (UTS), yield strength, and ductility of the steel wire samples are decreased by plasma hydrogenation and prestressing levels. The more drastic decrease in the UTS, yield strength, and ductility is found in the plasma hydrogenated prestressing steel to a higher prestressing level. Moreover, the hydrogen embrittlement index of the steel wire samples is significantly increased by plasma hydrogenation and prestressing level. The highly plasma hydrogenated prestressing steel wire samples exhibit complete brittle fracture. A mixed mode of fracture, i.e., ductile and brittle, was observed at the surface of the plasma hydrogenated prestressing steel wire samples at lower levels. The hydrogen embrittlement areas at the fracture surfaces of steel wire samples are observed to increase with plasma hydrogenation and prestressing levels. More severe hydrogen cracking and blistering resulted in the fracture surfaces of plasma-hydrogenated prestressing steel wire samples with higher levels.

Keywords: *Plasma hydrogenation, hydrogen embrittlement, high-carbon steel wire, prestressing.*

1. Introduction

The prestressing of the high-carbon steel wires impeded in concrete structures is applied to balance the tensile strength and to avoid the risk of failure of the concrete structures. The steel wire can be strain-hardened by cold drawing in several passes to increase its tensile strength[1]. Desirable stresses are introduced into the high-carbon structural steel wires by prestressing to counterbalance the undesirable stresses[2]. The high-strength steels are more susceptible to hydrogen embrittlement (HE)[3]. It was found that the application of a high-stress level of 70% of the ultimate tensile strength of the steel wire enhances the susceptibility of the hydrogen embrittlement induced by stress. The amount of hydrogen generated by the cathodic reaction plays an important role in the rupture of the prestressing steel under considerable mechanical stresses applied to the material[4].

Hydrogen embrittlement of steel occurs when hydrogen permeates and diffuses into steel in the prestressing steel wire by the classically proposed mechanism[5]. Non-ductile fracture mode is caused by hydrogen embrittlement, which reduces the ductility and tensile strength of steel[6]. The hydrogen embrittlement can lead to fracture if the steel is stressed in the presence of a hydrogen environment. It has been observed that the higher concentration of stresses at the crack tip leads to higher hydrogen concentrations accumulated at the crack tip. Moreover, hydrogen can accumulate at the interface

with the solution or at grain boundaries and cause brittle fractures[7]. Catastrophic failure of metallic materials showing brittle fracture behavior has resulted in the degradation of the mechanical properties[8]. The sensitivity of steel to hydrogen is manifested by both decreasing the yield strength and reducing the ductility. The decrease in the yield strength is attributed to the solid solution softening by hydrogen, whereas the reduction in the ductility is caused by the hydrogen-assisted fracture processes after the onset of necking[9]. It was found that the elongation to fracture of different types of steels is significantly reduced by hydrogen at room temperature, moreover, the introduction of hydrogen-enriched plasma at various temperatures into different kinds of steels degrades their mechanical properties by hydrogen embrittlement[10].

The steels having a tensile strength over 1200 MPa are more susceptible to hydrogen embrittlement, and the failure may occur at stresses much lower than their yield strength[11,12]. It was found that the susceptibility of prestressing steel wires to hydrogen embrittlement is high in cathodic environments[13]. The hydrogen embrittlement of the prestressing steel wires is attributed to the atomic hydrogen which is formed during the corrosion of steel. It is found that the susceptibility of the prestressing steel to hydrogen embrittlement is increased with increasing the amount of hydrogen trapped in the steel by defects such as grain boundaries and dislocations presented in the microstructure of the steel, moreover, the hydrogen embrittlement risk is attributed to the degradation mechanism, which can deform the metal lattice[14]. The diffusion of

*e-mail: amjadsalelamoush@gmail.com

hydrogen in X65 steel can be blocked by the defects, and as the concentration of hydrogen is increased in the steel, the risk of hydrogen embrittlement of the former steel is increased[15]. The dislocations were motivated by hydrogen plasma to contribute to crack formation in the ferritic alloys rather than forming local slip lines, and the cracks were formed inside the matrix of the specimen in a transgranular and brittle manner[16].

Hydrogen could be introduced into the prestressing steel during cathodic polarization by the hydrogen evolution reaction that occurred on the surface of steel at more negative potentials[17]. The loss of ductility or embrittlement is attributed to the penetrating atomic hydrogen into the prestressing steel wire during excessive cathodic production[18]. It was found that the hydrogen embrittlement of cold-drawn eutectoid steels has been caused by environmentally assisted cracking[19] and the highest-strength steel is the most susceptible to the hydrogen embrittlement[20]. The proposed mechanism of hydrogen-assisted failure in metals assumes that a critical couple of tensile stress and hydrogen concentration should have occurred at a finite-size material zone for failure initiation or propagation[21]. It has been observed that the mechanical strength of the steel wires is reduced by increasing the infiltration capacity of hydrogen, which results in hydrogen-induced cracking[22]. It was observed that the brittle zones are presented at the fracture surface of the prestressing steel, which is compatible with the presence of hydrogen[23]. The brittle fracture is occurred in high-strength steel because of the hydrogen adsorption in the steel structure[24]. Moreover, the results of the constant extension rate tensile tests reveal that the intergranular fracture mode has resulted from the increase of the hydrogen concentration in the ODS steel[25].

The current research investigates the effect of plasma hydrogenation on high-carbon prestressing structural steel wires. The tensile properties were evaluated by the SSRT to clarify the effects of both prestressing and plasma hydrogenation on the investigated material. Moreover, the fracture surfaces were examined by the scanning electron microscope (SEM) to determine the fracture morphology of the plasma-hydrogenated prestressing steel wires.

2. Experimental Procedure

The experiments were conducted on cold-drawn high-carbon steel wires of a diameter of 5mm and length of 200 mm. The chemical composition of the investigated material is listed in Table 1. The tensile tests were performed on the specimens cut from the steel wires and machined according to the E8/E8M-13a[26] as shown in Figure 1. The residual stresses induced by machining were removed by heating the tensile steel wire samples at a temperature of 200°C in an electric resistance furnace for 30 minutes. The high-carbon steel wire specimens were prestressed to different levels of 10%, 30%, 40%, 50%, 70%, and 85% of their ultimate tensile strengths in a plasma hydrogenation environment and then pulled in a slow strain rate test (SSRT). The tensile
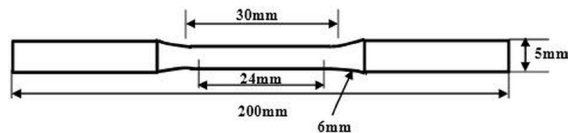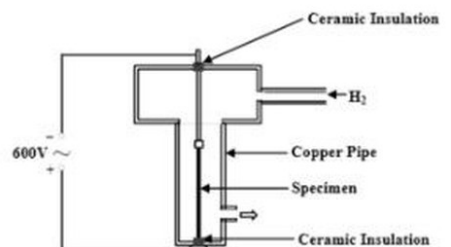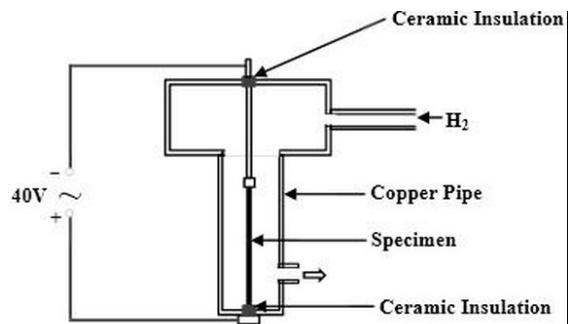
tests were performed by the universal testing machine at a constant crosshead speed of 1 mm/min. The elongations were measured by the extensometer with a gauge length of 24 mm as illustrated in Figure 1.

The plasma hydrogenation procedure of the prestressing steel wire specimens was performed in the hydrogen plasma gas at an ion current density of 20 mA cm^{-2} and a potential of 40V at the temperature of 130°C for 25 min. Hydrogen gas was introduced into the plasma chamber at a pressure of 10^{-5}Pa. The experimental setup for the plasma hydrogenation of the prestressing steel is shown in Figure 2.

The plasma-hydrogenated prestressing steel wire samples were pulled until fracture using SSRT at a strain rate of 10^{-6} s^{-1}. The strength and ductility were obtained from the stress-strain curves before and after plasma hydrogenation of the prestressing steel wire samples to various levels. The ductility of the steel wire samples was evaluated by the total elongation, i.e., the total strain to fracture. The modes

Figure 1. Tensile specimen dimensions designed according to the ASTM E8/E8M-13a[26].

Table 1. Chemical composition of the high carbon structural steel wire (wt%).

C	Mn	Si	Cu	P	S
0.83	0.69	0.21	0.27	0.011	0.0033

Figure 2. Schematic representation of the experimental setup used for hydrogen plasma charging of the prestressing steel wires.

of fracture of the plasma-hydrogenated prestressing steel wire samples were determined by SEM. The surfaces of the plasma-hydrogenated prestressing steel wire samples were observed by the SEM. The SEM samples were ground using abrasive paper with grit to 1200 and polished by diamond paste up to 1μm and then etched in 3% nital.

3. Results and Discussion

3.1. Microstructure of the steel wire

SEM observations of the surface of the as-received steel wire specimen reveal a fine pearlitic microstructure as shown in Figure 3a. This material is known as eutectoid steel containing 0.83% carbon. The pearlite colonies are consisting of cementite and ferrite lamellas as shown in Figure 3b.

3.2. Tensile behavior of the plasma-hydrogenated prestressing steel wires

The engineering stress-strain diagrams of the non-hydrogenated and plasma-hydrogenated prestressing steel wire samples prestressed to various levels are plotted in Figure 4. Different tensile properties have resulted from both prestressing and plasma hydrogenation. The variations in the tensile properties of the steel wire samples are attributed to both prestressing conditions and plasma hydrogenation. The ultimate tensile strengths (UTS) of plasma-hydrogenated prestressing steel wire samples are varied with the prestressing levels. The SSRT results show significant changes in the UTS of the plasma-hydrogenated prestressing steel wire samples after prestressing to various levels as compared to the non-hydrogenated, 0% prestressing sample. The change in the
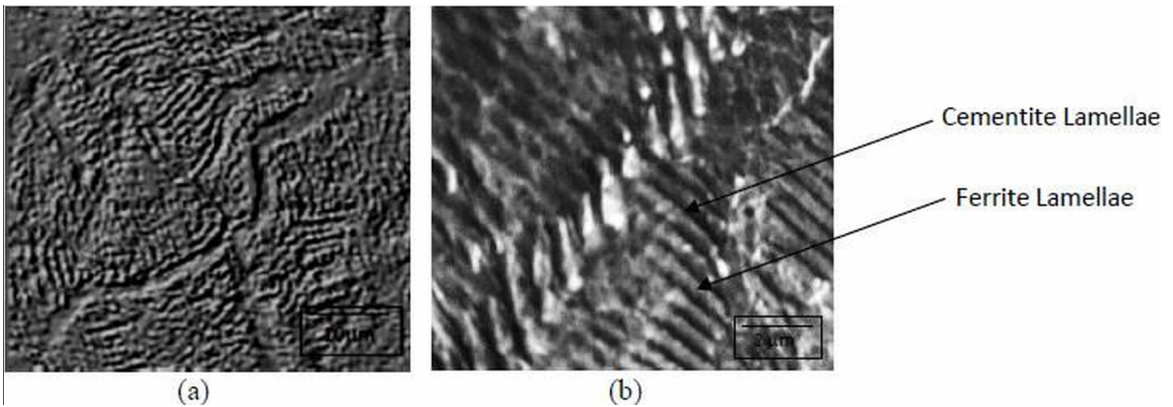

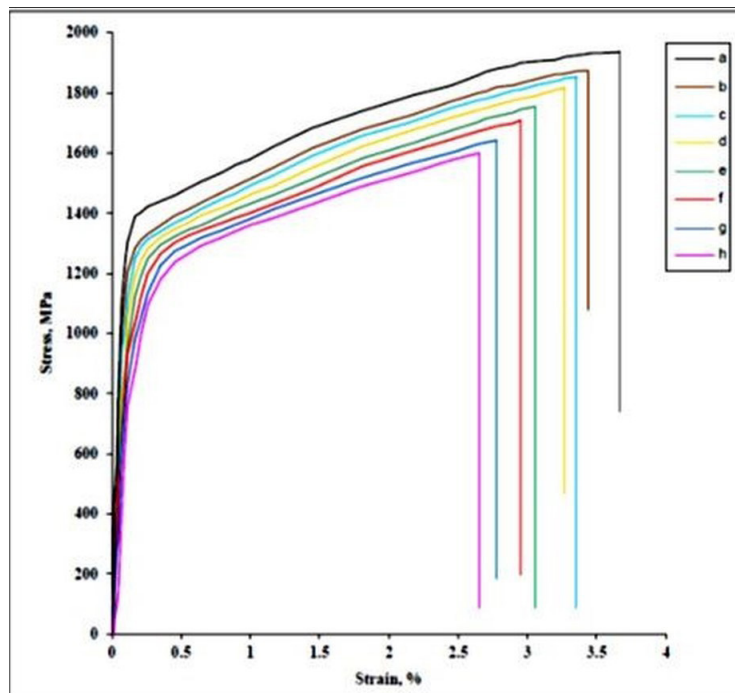**Figure 3.** Microstructure of the prestressing steel wire specimen.

Figure 4. Stress strain diagrams of the non-hydrogenated steel wire sample (a) and plasma-hydrogenated prestressing steel wire samples at a various level of: b) 0%, (c) 10%, (d) 30%, (e) 40%, (f) 50%, g) 70% and (h) 85%.

UTS depends on both plasma hydrogenation and prestressing levels applied to the steel wire samples.

The simultaneous effect of prestressing and plasma hydrogenation on the steel wire samples is shown in Figure 5. The results show that the prestressing and plasma hydrogenation decreases the UTS of the steel wire samples. The drop in the UTS is resulted from the ingress of plasma hydrogen during prestressing of steel wire samples. The hydrogen plasma flow rate is about 250ml/min from the hydrogen generator[16] and the measured density of plasma hydrogen atom is 2.5×10^{21} atom/m³ [27] which is expected to cause hydrogen embrittlement in the materials. Table 2 summarizes the tensile characteristics of the plasma-hydrogenated prestressing steel wire samples at different levels. As can be obtained from this table, the UTS of the plasma-hydrogenated prestressing steel wire sample with 10% is about 1853MPa, which is also lower than that of the non-hydrogenated and 0% prestressing steel wire sample (approximately 1930MPa). The decrease in the UTS of the plasma-hydrogenated prestressing steel wire sample to 10% is about 3.4% of the UTS of the non-prestressing steel wire sample. This slight decrease in the UTS is due to the above prestressing levels generating fewer trapping sites for hydrogen diffusion and building upon them. The further experimental results reveal that the
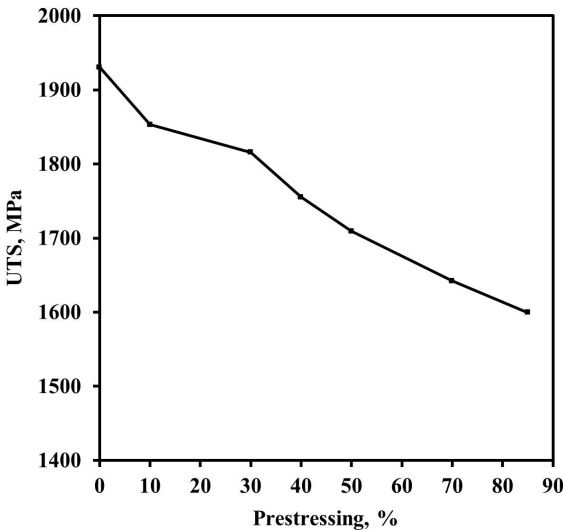
Figure 5. The UTS decrease in the plasma-hydrogenated prestressing steel wire samples to various levels.
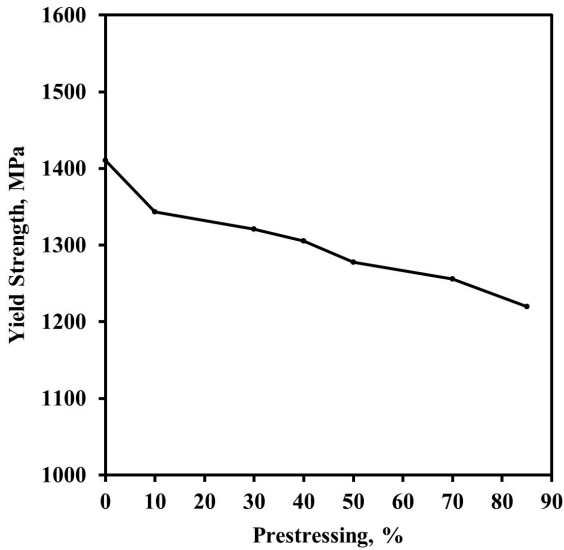
plasma-hydrogenated prestressing steel wire sample to a higher level (i.e., 30%) exhibits more decrease in UTS which is about 5.9% lower than that of the non-prestressing steel wire sample. The decrease in the UTS is found to be a unique function of both plasma hydrogenation and prestressing levels applied to the steel wires. The percentage decrease in the UTS is increased with both plasma hydrogenation and a prestressing level applied to the steel wire samples. The highest percentage decrease in the UTS was found in the plasma-hydrogenated prestressing steel wire samples with the highest level (i.e., 85%), which is about 17.1% of the UTS of the non-prestressing steel wire sample.

The degradation in the UTS of the plasma-hydrogenated prestressing steel wire samples is believed to be due to the lattice defects such as dislocations, grain boundaries, and vacancies generated during the prestressing of the steel wire samples where the hydrogen can build up at these defects and result in a drastic decrease in the UTS. These lattice defects can act as a strong trapping site for hydrogen absorption during plasma hydrogenation of the steel wire samples. It is believed that the highest level of prestressing (i.e.,85%) generates more dislocations, grain boundaries, and vacancies which increase the trapping sites for hydrogen absorption. This results in a more drastic drop in the UTS of the plasma-hydrogenated prestressing steel wire samples. It has been confirmed that the absorbed hydrogen atoms by the steel are trapped at interfaces, dislocations, and other microstructural features[28]. Moreover, it was indicated that the hydrogen diffuses to the dislocations and vacancies induced by the maximum strain in the steel[29]. Furthermore, the dislocations, voids, and grain boundaries are traps for the diffusion of hydrogen[30]. The high-stress or strain areas are observed to be preferential diffusion paths for hydrogen[31].

The yield strength of the plasma-hydrogenated prestressing steel wire samples revealed similar degradation behavior to that of the tensile strength. It was found that the yield strength depends also on both plasma hydrogenation and prestressing levels applied to the steel wire samples. The percentage decrease in yield strength of the plasma-hydrogenated prestressing steel wire as a function of prestressing level is shown in Figure 6. It is seen clearly from these curves that the increase in the prestressing levels results in lowering the yield strength of the plasma-hydrogenated prestressing steel wire samples. The decrease in the YS of the plasma-hydrogenated prestressing steel wire sample to 10% is about 4.7% of that of the non-prestressed wire sample as can be

Table 2. Tensile characteristics of the plasma-hydrogenated prestressing steel wire samples.

Prestressing, %	UTS, MPa	YS, MPa	Ductility, %	Percentage Decrease in UTS, %	Percentage Decrease in YS, %	Embrittlement Index, %
Non-hydrogenated and 0% prestressing sample	1930.3	1410	3.66	0	0	0
10	1853.2	1343.2	3.36	3.4	4.7	5.6
30	1815.8	1320.6	3.27	5.9	6.3	8.15
40	1755.2	1305.6	3.05	9.1	7.4	14.3
50	1709.2	1277.5	2.95	11.5	9.4	17.1
70	1642.1	1255.4	2.77	15	11	22.1
85	1599.6	1219.5	2.65	17.1	13.5	25.6

Figure 6. The decrease in the yield strength of the plasma-hydrogenated prestressing steel wire samples to various levels.

obtained from Table 2. Whereas the plasma-hydrogenated prestressing steel sample with a higher level (i.e., 30%) shows an approximately 6.3% decrease in the YS. The decrease in the yield strength may be attributed to the formation of cracks and blisters associated with plasma hydrogenation of the prestressing steel wire samples. As can be seen from this figure, the plasma-hydrogenated prestressing steel wire samples at higher levels show a drastic decrease in yield strength. The more drastic decrease in the yield strength was found in the plasma-hydrogenated prestressing steel wire samples at higher levels. As can be obtained from this figure, the plasma-hydrogenated prestressing steel wire sample at the highest level (i.e.,85%) exhibits the highest percentage decrease in the YS, which is approximately 13.5%. This decrease in the yield strength indicates that more severe hydrogen damage is induced in the plasma-hydrogenated prestressing steel wire samples to the highest levels.

The decrease in the yield strength could be attributed to the residual stresses induced by the prestressing and the hydrogen damage resulting from plasma hydrogenation. The delayed cracking at stress below the yield strength[32] causes the degradation of the properties of the steel by hydrogen. Moreover, the causes for the delayed cracking in the steel could be attributed to the diffusion of hydrogen to the areas of residual stresses[33]. It has been proposed two mechanisms related to hydrogen caused a decrease in the yield stress and caused fast fracture at the ultimate tensile strength[34]. The hydrogen-enhanced macroscopic plasticity (HEMP) mechanism related to the decrease of the yield stress by hydrogen, attributed to hydrogen causing solid solution softening, hydrogen-facilitated macroscopic movement of significant dislocation masses, thereby decreasing the yield stress[35].

It was found that the effect of hydrogen on the ductility and stress level in dual-phase steel is increased with deformation, which is due to the hydrogen-trapping ability of the deformation[36]. Furthermore, the tensile residual stresses

presented on the surface or in the core of the prestressing steel wire decrease the yield strength[37]. The hydrogen transportation rate towards prospective rupture sites in the prestressing wire is influenced by the heterogeneous residual stress fields[38]. The ductility represented by the strain to failure of the plasma-hydrogenated prestressing steel wire samples to different levels was also investigated and compared to the non-hydrogenated and 0% prestressing sample. The ductility of the plasma-hydrogenated prestressing steel wire sample prestressed to 10% is reduced to about 3.44% as compared to the non-hydrogenated and 0% prestressing sample which is about 3.66% as can be obtained from Table 2. This indicates that both plasma hydrogenation and prestressing have a pronounced effect on the ductility of the steel wire samples. Furthermore, the ductility of the plasma-hydrogenated prestressing steel wire sample prestressed to a higher level (i.e., 30%) is found to be also lower than that of non-hydrogenated and 0% prestressing steel wire sample. While the plasma-hydrogenated prestressing steel wire samples at higher levels (i.e., 50% and 70%) exhibit more decrease in ductility which are about 2.95% and 2.77% respectively lower than the ductility of the non-prestressing steel wire sample as shown in Table 2.

The plasma-hydrogenated prestressing steel wire sample at the highest level (i.e., 85%) exhibits the lowest ductility among all other plasma-hydrogenated prestressing steel wire samples which is about 2.65%. The loss in ductility observed in the plasma-hydrogenated prestressing steel wire samples can be attributed to hydrogen damage such as cracking and blistering induced by plasma hydrogenation. The ductility loss confirms that the severity of the damage depends on both plasma hydrogenation and a prestressing level applied to the steel wire samples. The more severe the hydrogen damage, the more loss in the ductility of the steel wire samples. It was observed that the mobile hydrogen in dislocations plays a detrimental role in the hydrogen embrittlement susceptibility of steel[39]. Moreover, the reduced ductility and the increased brittle failure of the high-strength steels are attributed to the presence of hydrogen in the material[40].

The loss in ductility can be attributed also to the fact that the hydrogen atoms are produced on the surface of the metal during the formation of the hydrogen molecule. Atomic hydrogen may penetrate the steel prior to combination to form hydrogen gas, which results in a loss of ductility of the prestressing wire[18]. Moreover, it is believed that more lattice defects are generated by the higher prestressing levels, which result in a more severe decrease in ductility. These lattice defects served as a potential diffusion path for hydrogen trapping.
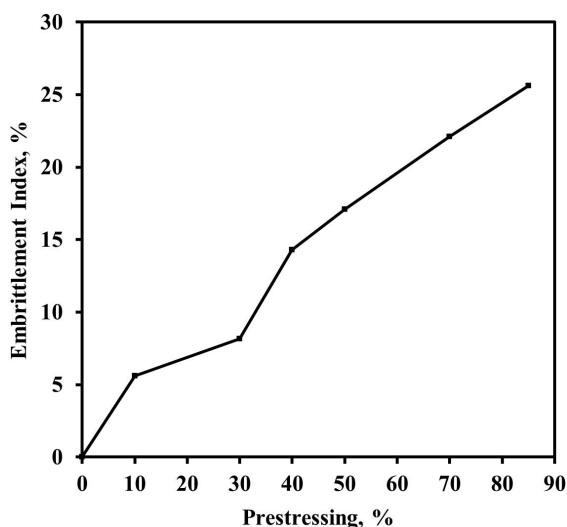
The hydrogen embrittlement index is calculated by the ductility loss[41]. From the tensile test results, the hydrogen embrittlement index I can be obtained from the differences in ductilities of the non-hydrogenated and plasma hydrogenated prestressing steel wire samples :

$$I = \frac{\varepsilon_{\text{unhy}} - \varepsilon_{\text{hypr}}}{\varepsilon_{\text{unhy}}} \times 100 \qquad (1)$$

Where $\varepsilon_{\text{unhy}}$ is the ductility of the non-hydrogenated, 0% prestressing steel wire sample and $\varepsilon_{\text{hypr}}$ is the ductility of the plasma-hydrogenated prestressing steel wire sample.

The results of calculations of the hydrogen embrittlement index for the plasma-hydrogenated prestressing steel wire samples are tabulated in Table 2. Figure 7 shows the hydrogen embrittlement index versus prestressing levels of the plasma-hydrogenated prestressing steel wire samples. It can be seen from this figure that the embrittlement index of the plasma-hydrogenated prestressing steel wire sample to a lower level of 10% has significantly reduced as compared to that of the non-hydrogenated and 0% prestressing steel wire sample. While the plasma-hydrogenated prestressing steel wire sample to a higher level (i.e., 30%) shows a further increase in the embrittlement index of about 8.15% as can be obtained from Table 2. Moreover, the highest value of the hydrogen embrittlement index is found for the plasma-hydrogenated prestressing steel wire sample at a higher level (i.e., 85%), which is about 25.6%. This finding implies that the former plasma-hydrogenated prestressing steel wire samples exhibit the highest sensitivity to hydrogen embrittlement among other plasma-hydrogenated prestressing steel wire samples to the lower levels. From these results, it is clearly seen that the embrittlement index is affected by both prestressing and plasma hydrogenation.

The sensitivity to hydrogen embrittlement of the steel wire was observed to increase with both plasma hydrogenation and prestressing levels as can be observed in Figure 7. The above finding can be attributed to the fact that the hydrogen trapping in steel wire samples was increased significantly by increasing the prestressing level, which generated more lattice defects such as grain boundaries, dislocations, voids, and other crystal defects. The molecular hydrogen is accumulated more in voids, pores, and interfaces than in other defect sites[42]. These defects are believed to increase with increasing the prestressing levels and thus increasing the potential trapping sites for hydrogen absorbing, which resulted in more severe degradation of the material. Furthermore, the accumulated hydrogen in the defects creates high pressure in them, which leads to the formation of new defects such as dislocations and vacancies[43].

Figure 7. The hydrogen embrittlement index of the plasma-hydrogenated prestressing steel wire samples as a function of prestressing.
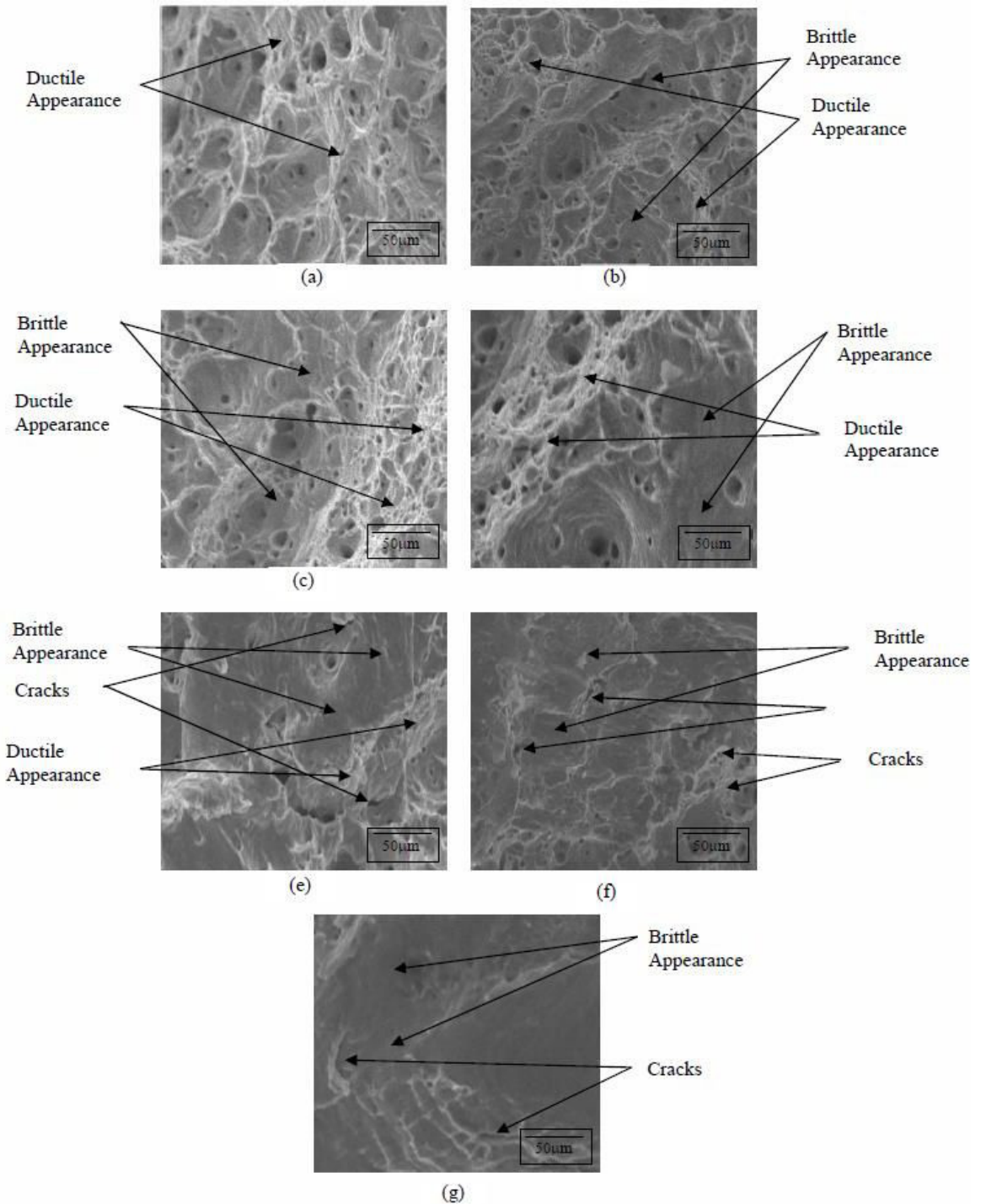
3.3. *Tensile fracture of the plasma-hydrogenated prestressing steel wires*

The plasma-hydrogenated prestressing steel wire samples have been pulled until fracture to determine the modes of the fracture using SEM. The fracture surface of the non-hydrogenated and 0% prestressing steel wire sample exhibited an entirely ductile appearance with dimples as can be seen in Figure 8a. However, the fractographic observations of the surface of the hydrogenated non-prestressing steel wire sample revealed mostly ductile with wide dimples and some areas of brittle appearance after the slow strain rate test (SSRT) as can be observed in Figure 8b. No significant changes in the fracture morphology of the plasma-hydrogenated prestressing steel wire samples to 10% level were observed which may be due to the insufficient hydrogen trapping sites caused by the above prestressing condition. While the fracture surface of the plasma-hydrogenated prestressing steel wire sample to a higher level (i.e., 30%) revealed two morphologies of fracture, namely, ductile, and brittle appearances as shown in Figure 8c). Moreover, narrow dimples were observed on the fracture surface of the plasma-hydrogenated prestressing steel wire samples. It is believed that the later prestressing condition results in more lattice defects such as dislocations and cracks, increasing the number of trapping sites for hydrogen diffusion and thus enhancing the susceptibility of the material to hydrogen embrittlement.

It is found that the stress and strain fields generated in the prestressing steel affect strongly the hydrogen diffusion towards prospective fracture sites[38], which may be also other causes for the hydrogen embrittlement. Moreover, the cleavage appearance in the brittle regions on the fracture surface of the prestressing steel wires is caused by the operation of hydrogen at the crack tip[44]. The hydrogen-induced brittle fracture was observed on ferritic steel after hydrogen plasma charging[45]. The cleavage-like failure is enhanced by lowering the free surface energy due to trapped hydrogen near the crack[46].

SEM observations of the fracture surfaces of the plasma-hydrogenated prestressing steel wire sample prestressed to a higher level (i.e., 40%) also revealed a mixed mode of fracture, i.e., ductile, and brittle appearances as can be observed in Figure 8d. However, the close examination of the fracture surface of the plasma-hydrogenated prestressing steel wire samples to 50% level showed larger embrittlement areas than those observed at the fracture surface of the plasma-hydrogenated prestressing steel wire samples to a lower level (i.e., 30%) as shown in Figure 8e. The hydrogen embrittlement areas at the fracture surfaces of the plasma-hydrogenated prestressing steel wire samples were observed to increase with increasing prestressing.

The hydrogen embrittlement areas at the fracture surfaces of the plasma-hydrogenated prestressing steel wire samples to 70% and 85% are larger than those at the fracture surfaces of the plasma-hydrogenated prestressing steel wire sample at a lower level as can be observed in Figure 8f and 8g. Furthermore, the experimental results show that the plasma-hydrogenated prestressing steel wire sample at the highest level (i.e., 85%) was fractured completely in a brittle manner with no evidence of ductile area in the whole fracture surface of the sample as can be seen in Figure 8g. It is seen clearly that the severity of the hydrogen embrittlement is increased

Figure 8. Fracture morphologies of the non-hydrogenated steel wire sample (a) and plasma-hydrogenated prestressing steel wire samples at various levels of: (b) 0%, (c) 30%, (d) 40%, (e) 50%, (f) 70% and (g) 85%.

by increasing the prestressing procedure, which indicates clearly that the susceptibility of steel wire samples to the hydrogen embrittlement is enhanced by both hydrogenation and prestressing levels.
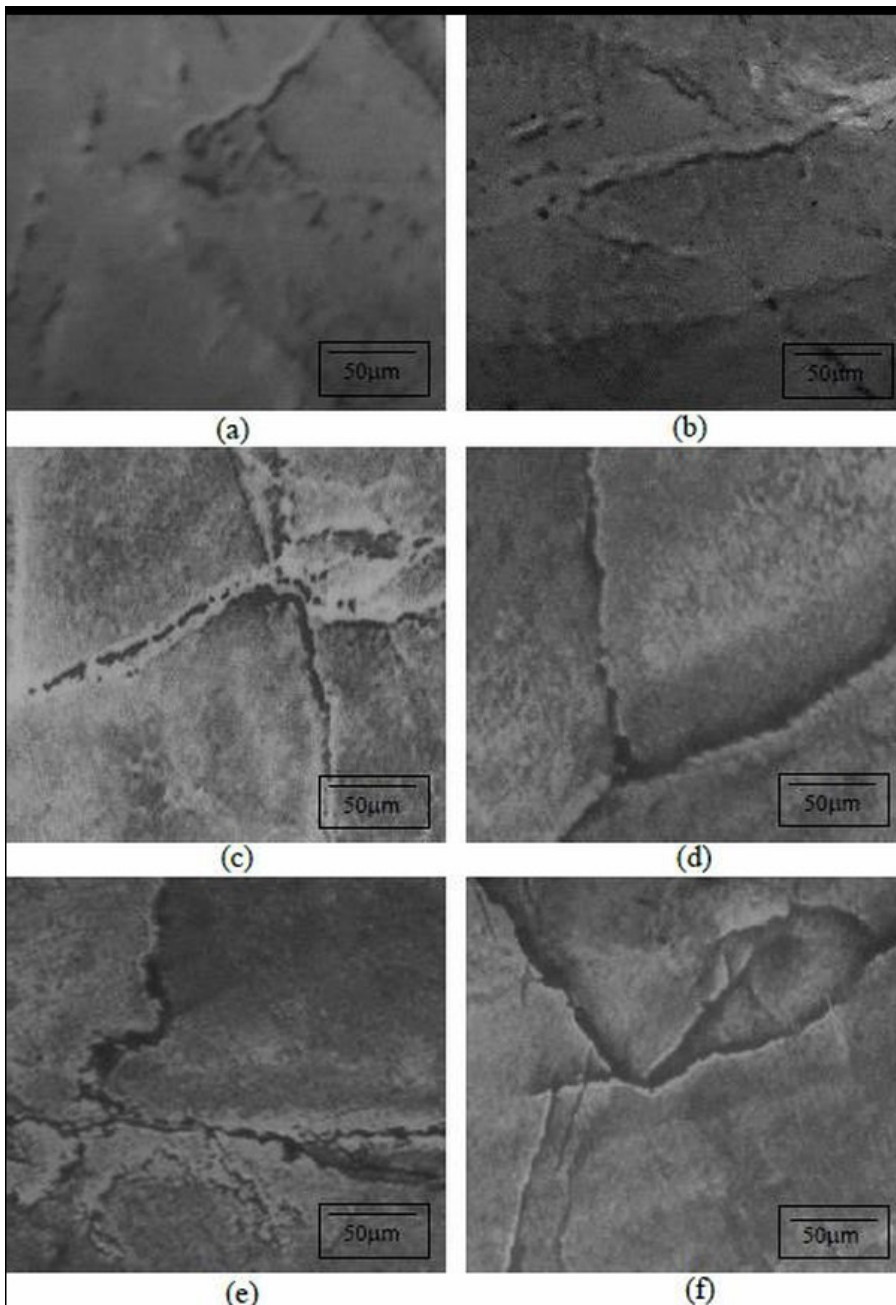
The evidence of hydrogen-assisted cracking was also noted at the fracture surfaces of the plasma-hydrogenated prestressing steel wire samples prestressed to various levels.

The experimental observations show that the prestressing enhances the hydrogen-assisted cracking in the steel wire samples. To further investigate the hydrogen-assisted cracking, SEM micrographs were taken from the fracture surfaces of the plasma-hydrogenated prestressing steel wire samples before and after prestressing. The SEM observations reveal that few and narrow hydrogen cracks are observed at the fracture

surfaces of the plasma-hydrogenated prestressing steel wire samples at a level of 30%. Whereas the plasma-hydrogenated prestressing steel wire samples to higher levels (i.e., 40% and 50%) showed more increase in the number of hydrogen cracks as can be seen from Figure 9c and 9d. In addition to these observations, the hydrogen cracks became longer on the fracture surfaces of the later plasma-hydrogenated prestressing steel wire samples compared to those observed on the fracture surface of plasma-hydrogenated prestressing steel wires at lower levels as revealed in Figure 9b.

The severity of the hydrogen cracking was observed to be enhanced with plasma hydrogenation and prestressing levels applied to the steel wire samples. The fracture surface of the plasma-hydrogenated prestressing steel wire sample to higher levels (i.e., 70% and 85%) revealed larger cracks than those observed on the fracture surface of the plasma-hydrogenated prestressing steel wire samples to lower levels of 30% to 50% as shown in Figure 9e and 9f. The hydrogen-induced cracking in steel can be explained by the diffusion of hydrogen atoms to the matrix interfaces and inclusions where the free energy is low, then the hydrogen molecules are formed from hydrogen atoms and built-up pressure on the material causing cracks[47]. Hydrogen cracks are formed along grain boundaries or other lattice defects in steel without


Figure 9. Hydrogen-assisted cracking on the fracture surfaces of the plasma-hydrogenated prestressing steel wire samples to: (a) 0%, (b) 30%, (c) 40%, (d) 50%, (e) 70% and (f) 85%.

externally applied stress by high concentrations of hydrogen trapped in the steel[48].

Hydrogen blisters are also observed on the fracture surfaces of the plasma-hydrogenated prestressing steel wire samples, the severity of which depends on the plasma hydrogenation and prestressing conditions applied to the material. The SEM observations of hydrogen blistering in the plasma-hydrogenated prestressing steel wire samples are shown in Figure 10. The plasma-hydrogenated prestressing steel wire sample to a lower level of 30% showed a few small blisters on its fracture surface as can be observed in Figure 10b. Whereas the hydrogen blisters in the plasma-hydrogenated prestressing steel wire samples to the highest levels of 40% and 50% as shown in Figure 10c and 10d) are observed to be larger and higher in number than those observed in the plasma-hydrogenated prestressing steel wire samples to a lower level of 30% as shown in Figure 10b. The experimental results confirm that the severity of hydrogen blistering is increased by plasma hydrogenation and prestressing levels applied to the steel wire samples. Furthermore, extensive hydrogen blisters are formed on the surface of the plasma-hydrogenated prestressing steel wire samples with the highest levels of 70% and 85% as can be observed in Figure 10e and 10f. Many experimental
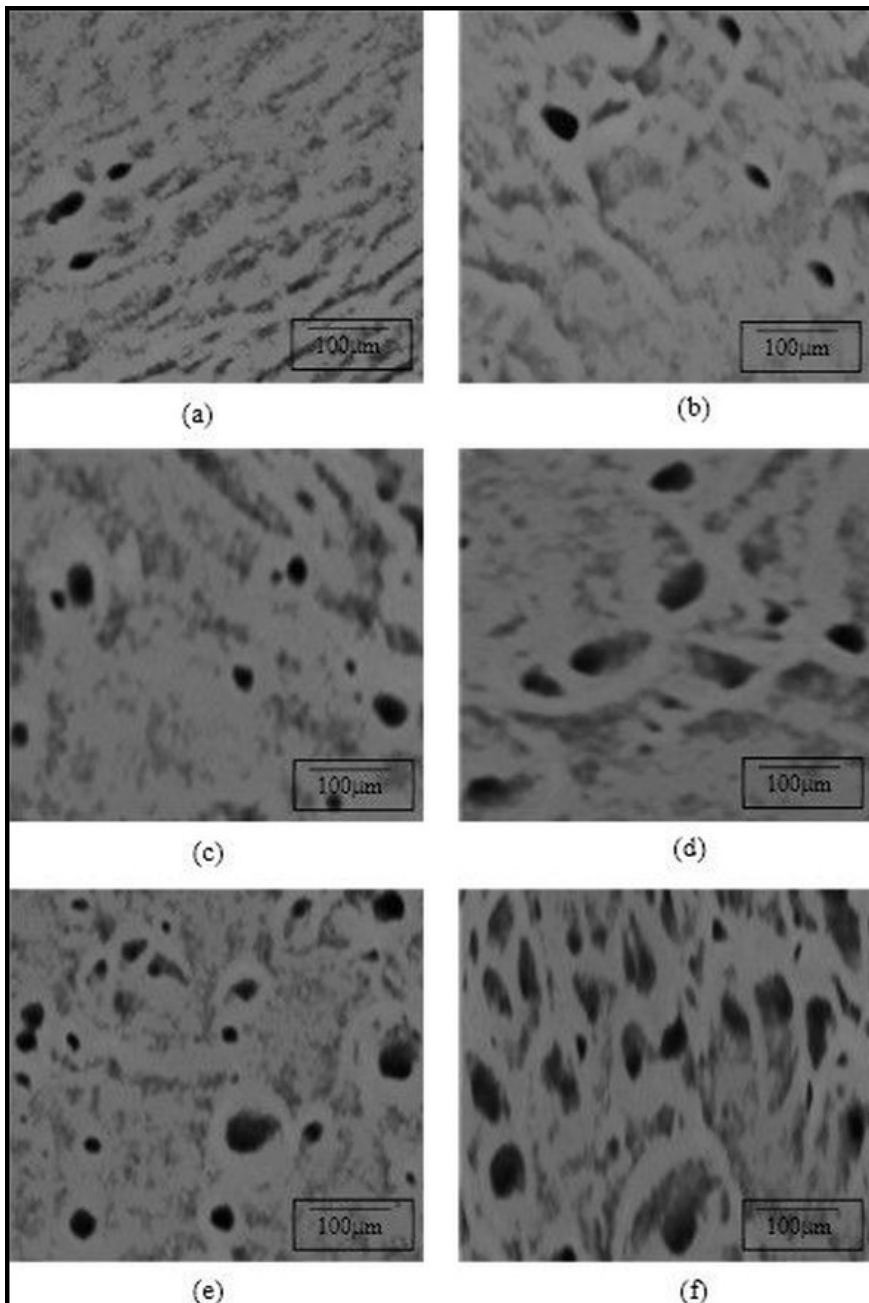
Figure 10. Hydrogen induced blistering on the surfaces of high carbon prestressing steel wire samples with: (a) 0%, (b) 30%, (c) 40%, (d) 50%, (c) 70% and (f) 85% and then plasma hydrogen charged.

investigations show similar behavior which is believed to be due to the increasing trap density for hydrogen resulting in the increasing number of hydrogen blisters on the steel surface[49].

Moreover, the main cause of hydrogen blisters is the formation of molecular hydrogen by the combination of atomic hydrogen[50]. It is also believed that as the trap density increased, the number of hydrogen blisters on the steel surface increased[51]. Moreover, A linear relationship has existed between the hydrogen trap density and the dislocation density[52]. The pressure builds up by the hydrogen molecules at the local deformation generated by the prestressing and a blister is formed at these deformed regions. The prestressing to the highest levels results in more localized deformed areas at which more hydrogen pressure builds up and forms extensive hydrogen blisters in the steel wire samples. As a result, the hydrogen blisters in the plasma-hydrogenated prestressing steel wire samples prestressed to the highest levels, are increased in number, and become large, which indicates that the plasma-hydrogenated prestressing steel wire samples prestressed to the highest levels are more susceptible to hydrogen-induced blistering than those steel wire samples prestressed to the lower levels.

4. Conclusions

The plasma hydrogenation of high-carbon prestressing steel wires was studied throughout the current investigation. The following concluding remarks can be made from the current research:

1. The plasma hydrogenation and prestressing have a significant effect on the tensile behavior of high-carbon steel wires. The plasma hydrogenation and the prestressing level lower the tensile properties of the steel wires.
2. The susceptibility of the steel wires is increased by both plasma hydrogenation and prestressing levels as it is indicated by the embrittlement index.
3. The plasma-hydrogenated prestressing steel wires prestressed to higher levels showed a complete brittle fracture, while the plasma-hydrogenated prestressing steel wire samples at lower levels showed the mixed mode of fracture, i.e., ductile, and brittle morphologies.
4. The more severe cracking and blistering are observed on the surfaces of the plasma-hydrogenated prestressing steel wire specimens to the highest level.

5. References

1. Toribio J, Ovejero E. Failure analysis of cold drawn prestressing steel wires subjected to stress corrosion cracking. Eng Fail Anal. 2005;5:654-61.
2. Valiente A, Slices M. Premature failure of prestressed steel bars. Eng Fail Anal. 1998;5:219-27.
3. Wang M, Akiyama E, Tsuzaki K. Effect of hydrogen on the fracture behavior of high strength steel during slow strain rate test. Corros Sci. 2007;49:4081-97.
4. Schroeder RM, Müller IL. Stress corrosion cracking and hydrogen embrittlement susceptibility of a eutectoid steel employed in prestressed concrete. Corros Sci. 2003;45:1969-83.
5. Price SM. The effect of sulphides on the passivity, crevice corrosion and hydrogen embrittlement of steel prestressing tendons. In: Proceedings of the International Congress on Metallic Corrosion; 1984 Jun 3-7; Toronto. Proceedings. Montreal: National Research Council of Canada; 1984. p. 262-9.
6. Nelson HG. Hydrogen embrittlement. In: Briant CL, Banerji SK, editors. Treatise on material science and technology. Vol. 25. New York: Academic Press; 1983. p. 275-359.
7. Pfeil L. The effect of occluded hydrogen on the tensile strength of iron. Proc Royal Soc, Math Phys Eng Sci. 1926;112(760):182-95.
8. Lynch S. Hydrogen embrittlement phenomena and mechanisms. Corros Rev. 2012;30:105-23.
9. Liu Q, Qingjun Z, Venezuela J, Zhang M, Atrens A. Hydrogen influence on some advanced high-strength steels. Corros Sci. 2017;125:114-38.
10. Malitckii E, Yagodzinskyy Y, Hänninen H. Hydrogen uptake from plasma and its effect on EUROFER 97 and ODS-EUROFER steels at elevated temperatures. Fusion Eng Des. 2015;98-99:2025-9.
11. Eliaz N, Shachar A, Tal B, Eliezer D. Characteristic of hydrogen embrittlement, stress corrosion cracking and tempered martensite embrittlement in high-strength steels. Eng Fail Anal. 2002;9:176-84.
12. Zhang YJ, Zhou C, Hui WJ, Dong H. Effect of C content on hydrogen induced delayed fracture behavior of MnB type steels. J Iron Steel Res. 2014;26:49-55.
13. Enos DG, Williams AJ, Scully JR. Long-term effects of cathodic protection of prestressed concrete structures: hydrogen embrittlement of prestressing steel. Corrosion. 1997;53:891-908.
14. Castellote M, Fullea J, Viedma PG, Andrade C, Alonso C, Liórente I et al. Hydrogen embrittlement steel submitted to slow strain rate studied by nuclear resonance reaction analysis and neutrón diffraction. Nucl Instrum Methods Phys Res B. 2007;259(2):975-83.
15. Liu Y, Gao Z, Lu X, Wang L. Effect of temperature on corrosion and cathodic protection of X65 pipeline steel in 3.5% NaCl solution. Int J Electrochem Sci. 2019;14:150-60.
16. Wan YDD, Barnoush A. Hydrogen embrittlement effect observed by in-situ hydrogen plasma charging on a ferritic alloy. Scr Mater. 2018;151:24-7.
17. Hope BB, Poland JS. Cathodic protection and hydrogen generation. ACI Mater J. 1990;87:469-72.
18. Sylvia C, Hall PE. Cathodic protection criteria for prestressed concrete pipe. In: Corrosion 98; 1998 Mar; San Diego. Proceedings. Houston: National Association of Corrosion Engineers; 1998. p. 98637.
19. Enos DG, Scully JR. A critical-strain criterion for hydrogen embrittlement of cold-drawn ultrafine pearlitic steel. Metall Mater Trans, A Phys Metall Mater Sci. 2002;33:1151-66.
20. Toribio J, Lancha AM. Effect of cold drawing on susceptibility to hydrogen embrittlement of prestressing steel. Mater Struct. 1993;26:30-7.
21. Serebrinsky S, Carter EA, Ortiz MJ. A quantum-mechanically informed continuum model of hydrogen embrittlement. J Mech Phys Solids. 2004;52:2403-30.
22. Wang SQ, Zhang DK, Wang DG. Xu1 LM, Ge1 SR. Stress corrosion behaviors of steel wires in coalmine under different corrosive mediums. Int J Electrochem Sci. 2012;7:7376-89.
23. Sanchez J, Fullea J, Andrade C, Alonso C. Stress corrosion cracking mechanism of prestressing steels in bicarbonate solutions. Corros Sci. 2007;49:4069-80.
24. Nurnberger U. Corrosion induced failures of prestressing steel. Otto Graf J. 2002;13:9-26.
25. Yagodzinskyy Y, Malitckii E, Ganchenkova M, Binyukova S, Emelyanova O, Saukkonen T et al. Hydrogen effects on tensile properties of EUROFER 97 and ODS-EUROFER steels. J Nucl Mater. 2014;444(1-3):435-40.

26. ASTM: American Society for Testing and Materials. ASTM E8/E8M-13a: standard test methods for tension testing of metallic materials. West Conshohocken: ASTM; 1996.

27. Vesel A, Drenik A, Zaplotnik R, Mozetic M, Balat-Pichelin M. Reduction of thin oxide films on tungsten substrate with highly reactive cold hydrogen plasma. Surf Interface Anal. 2010;42(6-7):1168-71.

28. Dong CF, Liu ZY, Li XG, Cheng YF. Effects of hydrogen-charging on the susceptibility of X100 pipeline steel to hydrogen-induced cracking. Int J Hydrogen Energy. 2009;34:9879-84.

29. Bao YB. Dependence of ductile crack formation in tensile tests on stress triaxiality, stress and strain ratios. Eng Fract Mech. 2005;72:505-22.

30. Depover T, Wallaert E, Verbeken K. Fractographic analysis of the role of hydrogen diffusion on the hydrogen embrittlement susceptibility of DP steel. Mater Sci Eng A. 2016;649:201-8.

31. Timmins PF. Solutions to hydrogen attack in steels. Russel: ASM International; 1997.

32. Turnbull A. Perspectives on hydrogen uptake, diffusion, and trapping. Int J Hydrogen Energy. 2015;40(47):16961-70.

33. Zinbi A, Bouchou A. Delayed cracking in 301 austenitic steel after bending process: martensitic transformation and hydrogen embrittlement analysis. Eng Fail Anal. 2010;17(5):1028-37.

34. Liu Q, Zhou Q, Venezuela J, Zhang M, Atrens A. Hydrogen influence on some advanced high-strength steels. Corros Sci. 2017;125:114-38.

35. Venezuela J, Zhoub Q, Liua Q, Lia H, Zhang M, Matthew SD, et al. The influence of microstructure on the hydrogen embrittlement susceptibility of martensitic advanced high strength steels. Mater Today Commun. 2018;17:1-14.

36. Depover T, Hajilou T, Wan D, Wang D, Barnoush A, Verbeken K. Assessment of the potential of hydrogen plasma charging as compared to conventional electrochemical hydrogen charging on dual phase steel. Mater Sci Eng A. 2019;754:613-21.

37. Atienza JM, Ruiz-Hervias J, Caballero L, Elices M. Residual stresses and durability in cold drawn eutectoid steel wires. Met Mater Int. 2006;13:139-43.

38. Toribio J, Elices M. Influence of residual stresses on hydrogen embrittlement susceptibility of prestressing steels. Int J Solids Struct. 1991;28:791-803.

39. Depover T, Verbeken K. The detrimental effect of mobile hydrogen at dislocations on the hydrogen embrittlement susceptibility of Fe-C-X alloys: an experimental proof of the HELP mechanism. Int J Hydrogen Energy. 2018;43:3050-61.

40. Ćwiek J. Hydrogen degradation of high-strength steels. J Achiev Mater Manuf Eng. 2009;2(37):193-212.

41. Ping T, Fei Y, Weiwei C, Jiaxi Z, Yanfei W, Jianming G. Analysis of enhanced hydrogen embrittlement fracture for pre-strain hardening 2205 duplex stainless steel. Results Phys. 2020;16:102820.

42. Mallick A, Das S, Mathur J, Bhattacharyya T, Dey A. Internal reversible hydrogen embrittlement leads to engineering failure of cold drawn wire. Case Stud Eng Fail Anal. 2013;1:139-43.

43. Pavlyna VS, Pavlyna OV. Hydrogen permeability in metals under the conditions of accumulation of defects. Mater Sci. 2007;43(5):597-607.

44. Vehovar L, Kuhar V, Vehovar A. Prestressing wires in a motorway viaduct. Eng Fail Anal. 1998;1:21-7.

45. Wan D, Deng Y, Barnoush A. Hydrogen embrittlement effect observed by in-situ hydrogen plasma charging on a ferritic alloy. Scr Mater. 2018;151:24-7.

46. Xing X, Yu M, Chen W, Zhang H. Atomistic simulation of hydrogen-assisted ductile-to-brittle transition in α-iron. Comput Mater Sci. 2017;127:211-21.

47. Krom AHM, Bakker A. Modeling Hydrogen-induced Cracking in Steel Using a Coupled Diffusion Stress. Int J Press Vessels Piping. 1997;72:139-47.

48. Mohtadi-Bonab MA, Szpunar JA, Razavi-Tousi SS. A comparative study of hydrogen induced cracking behavior in API 5L X60 and X70 pipeline steels. Eng Fail Anal. 2013;33:163-75.

49. Park GT, Koh SU, Jung HG, Kim KY. Effect of microstructure on the hydrogen trapping efficiency and hydrogen-induced cracking of linepipe steel. Corros Sci. 2008;50:1865-71.

50. Ren XC, Zhou QJ, Shan GB, Chu WY, Li JX, Su YJ, et al. A nucleation mechanism of hydrogen blister in metals and alloys. Metall Mater Trans, A Phys Metall Mater Sci. 2008;39:87-97.

51. Huang F, Liu J, Deng ZJ, Cheng JH, Lu ZH, Li XG. Effect of microstructure and inclusions on hydrogen-induced cracking susceptibility and hydrogen trapping efficiency of X120 pipeline steel. Mater Sci Eng A. 2010;527:6997-7001.

52. Yen SK, Huang IB. Critical hydrogen concentration for hydrogen-induced blistering on AISI 430 stainless steel. Mater Chem Phys. 2003;80:662-6.